



**Colorimetric and Fluorescent detection of G-quadruplex Nucleic Acids with a Coumarin-benzothiazole Probe**

Journal:	<i>Analyst</i>
Manuscript ID:	AN-COM-08-2015-001573.R1
Article Type:	Communication
Date Submitted by the Author:	21-Aug-2015
Complete List of Authors:	Yan, Jin-Wu; South China University of Technology, School of Bioscience and Bioengineering; Sun Yat-sen University, Guangdong Provincial Key Laboratory of New Drug Design and Evaluation, School of Pharmaceutical Science Tian, Yi-Guang; South China University of Technology, School of Bioscience and Bioengineering Tan, Jia-Heng; Sun Yat-sen University, School of Pharmaceutical Sciences Huang, Zhi-Shu; Sun Yat-sen University, School of Pharmaceutical Sciences

Cite this: DOI: 10.1039/c0xx00000x

www.rsc.org/xxxxxx

## COMMUNICATION

## Colorimetric and Fluorescent detection of G-quadruplex Nucleic Acids with a Coumarin-benzothiazole Probe

Jin-wu Yan,<sup>\*ab</sup> Yi-guang Tian,<sup>a</sup> Jia-heng Tan<sup>b</sup> and Zhi-shu Huang<sup>b</sup>

Received (in XXX, XXX) Xth XXXXXXXXXX 20XX, Accepted Xth XXXXXXXXXX 20XX

DOI: 10.1039/b000000x

A colorimetric and red-emitting fluorescent dual probe for G-quadruplex was devised with a conjugated coumarin-benzothiazole scaffold. Its significant and distinct changes in both color and fluorescence enable the label-free and visual detection of G-quadruplex structures. In addition, this probe gives a distinct strong emission response to the nucleoli in the fixed cells imaging, which might be attribute to the interaction between the probe with rDNA G-quadruplex based on the chromatin immunoprecipitation assay. All these results suggest its promising application prospects in G-quadruplex research field.

G-Quadruplexes are unique four-stranded structures adopted by repetitive guanine-rich sequences in many crucial genomic regions.<sup>1, 2</sup> Analysis of the human DNA has revealed an abundance of putative G-quadruplex-forming sequences (PQSs) in the human genome, such as telomeric DNA, promoter region of some oncogenes and RNA sequences.<sup>2</sup> During the past two decades, G-quadruplex structures have captivated huge attention because of their biological significance and potential applications in nanotechnology and supramolecular chemistry,<sup>3-8</sup> which necessitate the development of rapid and facile approaches for the sensitive and selective detection of this secondary structure. In recent years, great efforts have been made to develop probes for the detection of G-quadruplex in vitro and in vivo, and many probes have been reported, including organic molecules, metal complexes and nanoparticles.<sup>9-17</sup> Colorimetric detection with visible color changes is very attractive due to the advantage of simplicity and low cost. However, one of the common limitations of colorimetric detection is that it can only be utilized *in vitro*.

<sup>a</sup> School of Bioscience and Bioengineering, South China University of Technology, Guangzhou, P. R. China.

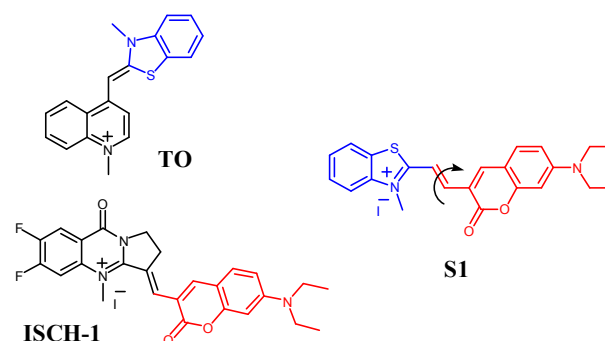
<sup>b</sup> Guangdong Provincial Key Laboratory of New Drug Design and Evaluation, School of Pharmaceutical Science, Sun Yat-sen University, Guangzhou 510006, China.  
E-mail: yjw@scut.edu.cn.

<sup>†</sup> Electronic Supplementary Information (ESI) available: Synthesis and characterization of **S1**, experimental procedures, and supplemental spectra and graphs.

As we know, the existence and function of G-quadruplex structures in mammalian cells remains controversial, thus the design of specific fluorescent probes with long-wavelength excitation for detecting and monitoring G-quadruplex structures in cells is in great demand.

To date, most of the G-quadruplex probes exhibited only one kind of output, such as colorimetric, fluorescent or electrochemical signals, thus it would be highly valuable to develop probes that provide a combination of different outputs. In this study, we present a colorimetric and red-emitting fluorescent dual probe for G-quadruplexes based on coumarin-benzothiazole scaffold. This probe showed promising application in rapid, label-free and naked-eye detection of G-quadruplexes based on its significant and distinct response in both UV-vis absorption and fluorescence emission.

Coumarins are widely used as fluorescent labels for molecular studies of nucleic acids and proteins, and also as chemosensors for various anions and metal cations.<sup>18-22</sup> The structure of coumarin moiety has been extensively modified and studied with regard to their simple preparation process and favorable photophysical properties, such as high quantum yield, large Stokes shift and excellent photostability. Recently, we reported the colorimetric and fluorescent dual probe **ISCH-1** for G-quadruplex obtained by incorporating a coumarin fluorophore into an isaindigotone framework, which showed vivid color changes and significant fluorescence enhancement upon its incubation with G-quadruplexes.<sup>23</sup> On the other hand, benzothiazole-based molecules, such as



Scheme 1 Structures of probes TO, ISCH-1 and S1.

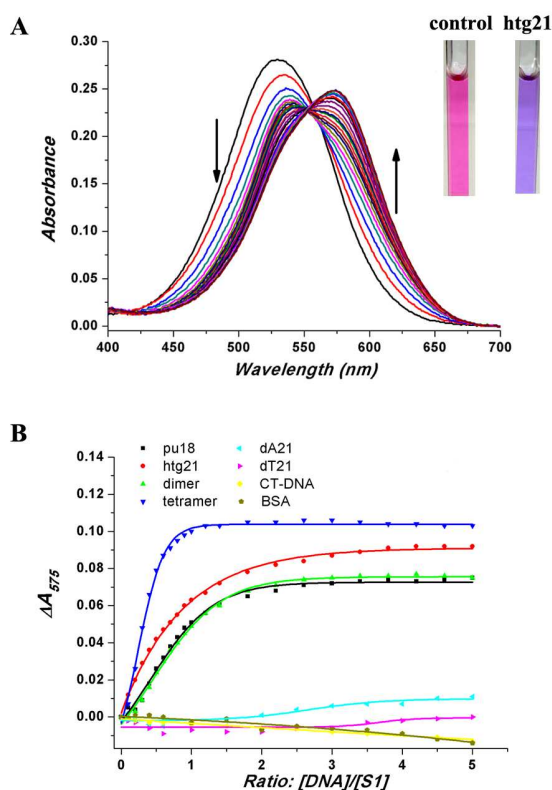


**Fig. 1** (A) UV-vis spectroscopic titration of **S1** by stepwise addition of G-quadruplex forming oligonucleotide (htg21). Conditions:  $[S1] = 5 \mu\text{M}$ ; 10 mM Tris-HCl buffer, 60 mM KCl, PH 7.4. The spectra were recorded at 1 min intervals. Inset: color changes upon addition of htg21. (B) The absorbance enhancement of 5 μM **S1** at 575 nm versus  $[DNA]/[S1]$  molar ratio.

thiazole orange (**TO**), have been widely used as fluorescent probes for DNA detection and intracellular DNA imaging.

Inspired by our previous study, we attempted to construct a new dual probe for G-quadruplex based on the push-pull probe architecture by incorporating a coumarin fluorophore with an N-methylated benzothiazole moiety into a fusion scaffold (**S1**, Scheme 1). The rotation of the methine-bridge would impact the push-pull effects between the coumarin moiety (donor) and the N-methylated benzothiazole moiety (acceptor), and consequently, it would influence the radiative pathway relaxation and fluorescence emission of **S1**. We anticipated that the rotation of **S1** may be restricted after binding to specific DNA structure, and give rise to different spectroscopy response, which could be utilized to distinguish the DNA structures. The desired probe **S1** was easily obtained by the condensation of the coumarin aldehyde with N-methyl-2-methylbenzothiazolium iodide (Scheme S1, ESI†). This probe was firstly reported for fluorescent detection of SO<sub>2</sub> derivatives based on their addition-rearrangement cascade reaction.<sup>24</sup> A widely used strategy to develop G-quadruplex probe is to study the G-quadruplex sensing ability of some reported fluorescent probes, which are used to detect other analytes. For example, Thioflavin T (ThT) has recently been reported as a turn-on fluorescent sensor for G-quadruplexes,<sup>25, 26</sup> which once was widely used in detect amyloid fibrils.<sup>27</sup> In

this study, we evaluated the interaction between **S1** with 35 different oligonucleotides to verify if it could be utilized as a specific probe for G-quadruplexes.

First, the UV-vis spectroscopic titrations were performed to investigate the interactions of our probe with G-quadruplex. **S1** exhibited a predominant absorption band at around 525 nm. Upon addition of a G-quadruplex forming oligonucleotide (htg21), the intensity at 525 nm gradually decreased, and a large red-shift (50 nm) of the absorption maximum could be observed with a isosbestic point at 550 nm (Fig. 1A), which eventually led to a new maximum at around 575 nm. The 45 specific red-shift induced by G-quadruplexes gave rise to a vivid color change from pink to purplish blue in ambient light. Then, we investigated the interaction between **S1** with different DNA sequences, including G-quadruplexes with different conformation, single and duplex strands and BSA 50 protein. As shown in Fig. 1B, G-quadruplexes including pu18, htg21, dimer and tetramer strands could enhance the absorbance at 575 nm. On the other hand, the absorbance of **S1** was slightly disturbed by single strands (dA21 and dT21), linear duplex CT-DNA (calf thymus DNA) and BSA protein 55 under the same conditions. These results indicated that G-quadruplexes could be easily and specifically detected with the naked eye by using **S1**.

Furthermore, the fluorescent properties of **S1** with different DNAs were explored by fluorescence titration. Free **S1**

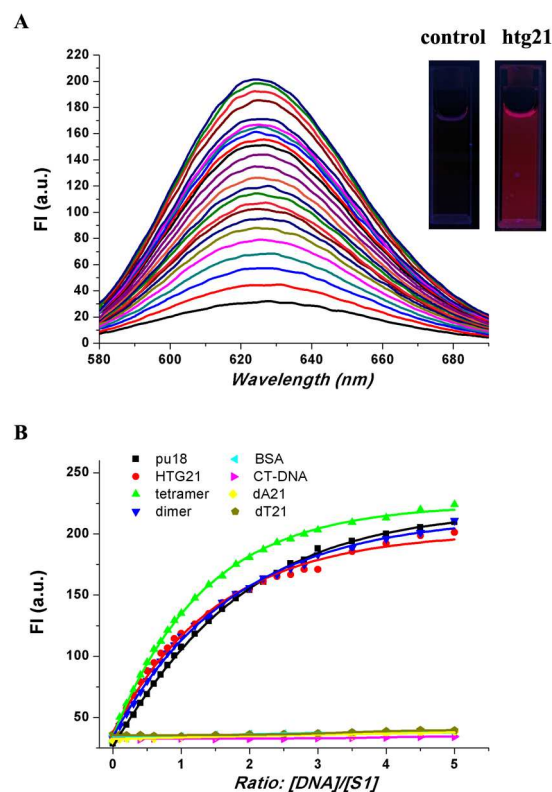


**Fig. 2** (A) Fluorescence titration of **S1** by stepwise addition of G-quadruplex forming oligonucleotide (htg21). Conditions:  $[S1] = 0.2 \mu\text{M}$ ; 10 mM Tris-HCl buffer, 60 mM KCl, PH 7.4. The spectra were recorded at 1 min intervals. (B) The fluorescence intensity enhancement of 0.2 μM **S1** at 625 nm versus  $[DNA]/[S1]$  molar ratio,  $\lambda_{\text{ex}} = 550 \text{ nm}$ .

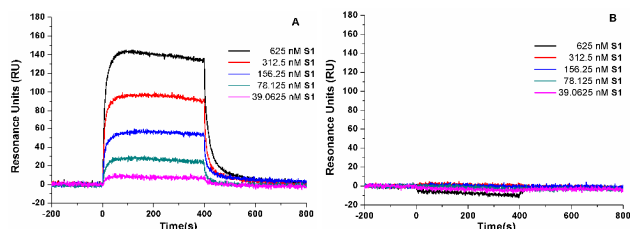


**Fig. 3** SPR sensorgram overlay for binding of **S1** to htg30 (A) and duplex DNA (B). The ligand concentrations in the flow solution are given in the figure.

displayed a weak emission at 625 nm with a quantum yield ( $\Phi_F$ ) of 0.032 and a short lifetime of 0.37 ns (Table S4 and Fig. S7). Upon titration with htg21, the emission intensity around 625 nm significantly enhanced with increasing htg21 concentrations (Fig. 2A). The corresponding  $\Phi_F$  and fluorescence lifetime also increased to 0.394 and 2.5 ns at the saturated concentration of htg21, respectively. We speculated that the interaction between **S1** and htg21 may restrict the rotation of the methine-bridge of **S1**, therefore enhancing the radiative pathway relaxation and fluorescence emission. It is worthy to point out that the long excitation and emission maxima of **S1** are very attractive for the cellular imaging experiments, as low photo-damage, and minimal fluorescence background can be achieved. We also investigated the selectivity of **S1** with different DNAs. As shown in Fig. 2B, the turn-on emission response of **S1** only occurred in the presence of G-quadruplexes, which indicated the excellent selectivity for G-quadruplex displayed by **S1**. The specific red fluorescence of **S1** with G-quadruplexes could also be observed by naked eye under UV light. As shown in Table S3, the detection limits (LOD) of **S1** for G-quadruplexes were around 10 nM, and the linear ranges of the fluorescence titration curve for the tested G-quadruplexes ranged from 0–120 to 0–200 nM.

The selectivity of **S1** for G-quadruplex was further demonstrated by using surface plasma resonance (SPR, Fig. 3). As shown in Table S2, **S1** exhibited excellent binding affinity to G-quadruplexes ( $K_D$ , 0.397–0.825  $\mu$ M), while no significant binding was found for addition of up to 10  $\mu$ M **S1** (Fig. S5), which might indicate no specific interactions between **S1** with the duplex-strand and single-strand DNA. Taking all these exciting results together, our probe **S1** displayed promising application prospects for selective and sensitive detection of G-quadruplex with colorimetric and fluorescent dual outputs.

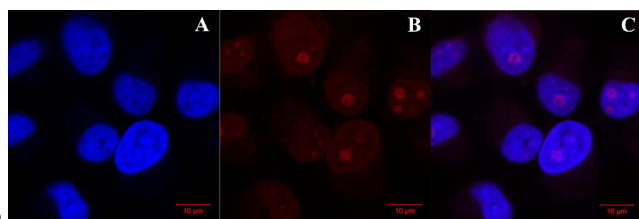


**Fig. 4** Confocal fluorescence images of fixed HeLa cells using a 543 nm laser. HeLa cells stained with 5  $\mu$ g/mL DAPI (A) for 30 min and 5  $\mu$ M **S1** (B) for 1 h and overlap field (C).

In addition, we further investigated the cellular application of

**S1** in fixed HeLa cells by using confocal laser scanning microscopy. Co-staining with DAPI revealed that our probe **S1** has a distinct strong emission in the nucleoli (Fig. 4), which contain abundant putative G-quadruplex forming sequences, including rDNA G-quadruplexes.<sup>28, 29</sup> In addition, weak fluorescence emission could be observed in the other region of nucleus, probably due to the non-specific interaction with the highly abundant duplex DNA.

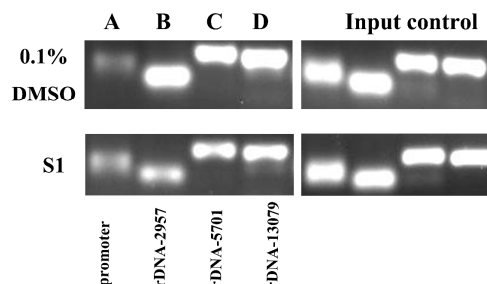


**Fig. 5** Chromatin immunoprecipitation analysis for the effect of **S1** on the interaction between the rDNA promoter region without PQS (A) and three PQS-containing regions (B–D) in the nontemplate strand of rDNA. A549 cells were treated with 10  $\mu$ M **S1** or 0.1% DMSO for 16 h.

To clarify whether **S1** can selectively bind to the rDNA G-quadruplexes in cells, we performed chromatin immunoprecipitation (ChIP) assay according to the procedure for an accepted rDNA G-quadruplex binder, CX-3543.<sup>29</sup> Three PQS-containing regions in the nontemplate strand of rDNA and one rDNA promoter region without PQS were selected for this assay, and nucleolin was used as the binding protein of rDNA. The result showed that the complexes between nucleolin and all three PQS-containing regions were obviously disrupted after treatment with **S1** (Fig. 5, lane B–D), especially for rDNA-2957. However, **S1** showed little effect on the interaction between nucleolin and rDNA promoter region without PQS (Fig. 5, lane A). All these results revealed that the intracellular binding target of **S1** might be rDNA G-quadruplex.

## Conclusions

To conclude, we demonstrated that the coumarin-benzothiazole hybrid probe **S1** can be used as a colorimetric and red-emitting fluorescent dual probe for specific and visual detection of G-quadruplexes, based on its significant absorbance shift and fluorescence enhancement in the presence of G-quadruplexes. The intracellular imaging ability of **S1** was investigated in fixed cells, and its distinct strong emission was observed in the nucleoli, which might be attributed to the interaction between **S1** with rDNA G-quadruplex. All these remarkable properties of this probe suggest that it should have promising application prospects in the field of G-quadruplex research.

This work was supported by the Fundamental Research Funds for the Central Universities (Grant No.: 2014ZB0002), and the Opening Project of Guangdong Provincial Key Laboratory of New Drug Design and Evaluation (Grant No.: 2011A060901014).

## Notes and references

1. M. Gellert, M. N. Lipsett and D. R. Davies, *Proc. Natl. Acad. Sci. U S A*, 1962, **48**, 2013-2018.
2. V. S. Chambers, G. Marsico, J. M. Boutell, M. Di Antonio, G. P. Smith and S. Balasubramanian, *Nat. Biotech.*, 2015, doi: 10.1038/nbt.3295.
3. D. S.-H. Chan, H. Yang, M. H.-T. Kwan, Z. Cheng, P. Lee, L.-P. Bai, Z.-H. Jiang, C.-Y. Wong, W.-F. Fong, C.-H. Leung and D.-L. Ma, *Biochimie*, 2011, **93**, 1055-1064.
4. H.-Z. He, K.-H. Leung, W. Wang, D. S.-H. Chan, C.-H. Leung and D.-L. Ma, *Chem. Commun.*, 2014, **50**, 5313-5315.
5. L. Parrotta, F. Ortuso, F. Moraca, R. Rocca, G. Costa, S. Alcaro and A. Artese, *Expert Opin. Drug Discov.*, 2014, **9**, 1167-1187.
6. S. Wang, B. Fu, J. Wang, Y. Long, X. Zhang, S. Peng, P. Guo, T. Tian and X. Zhou, *Anal. Chem.*, 2014, **86**, 2925-2930.
7. T. Tian, H. Xiao and X. Zhou, *Curr. Top. Med. Chem.*, 2015, **15**, 1988-2001.
8. M. Wang, B. He, L. Lu, C.-H. Leung, J.-L. Mergny and D.-L. Ma, *Biosens. Bioelectron.*, 2015, **70**, 338-344.
9. E. Largy, A. Granzhan, F. Hamon, D. Verga and M. P. Teulade-Fichou, *Top. curr. chem.*, 2013, **330**, 111-177.
10. H. Lai, Y. Xiao, S. Yan, F. Tian, C. Zhong, Y. Liu, X. Weng and X. Zhou, *Analyst*, 2014, **139**, 1834-1838.
11. D. Zhao, X. Dong, N. Jiang, D. Zhang and C. Liu, *Nucleic Acids Res.*, 2014, **42**, 11612-11621.
12. L. Lu, D. Shiu-Hin Chan, D. W. J. Kwong, H.-Z. He, C.-H. Leung and D.-L. Ma, *Chem. Sci.*, 2014, **5**, 4561-4568.
13. D.-L. Ma, S. Lin, K.-H. Leung, H.-J. Zhong, L.-J. Liu, D. S.-H. Chan, A. Bourdoncle, J.-L. Mergny, H.-M. D. Wang and C.-H. Leung, *Nanoscale*, 2014, **6**, 8489-8494.
14. M.-H. Hu, S.-B. Chen, R.-J. Guo, T.-M. Ou, Z.-S. Huang and J.-H. Tan, *Analyst*, 2015, **140**, 4616-4625.
15. A. C. Bhasikuttan and J. Mohanty, *Chem. Commun.*, 2015, **51**, 7581-7597.
16. D. L. Ma, M. Wang, S. Lin, Q. B. Han and C. H. Leung, *Curr. Top. Med. Chem.*, 2015, **15**, 1957-1963.
17. X. Xie, A. Renvoise, A. Granzhan and M.-P. Teulade-Fichou, *New J. Chem.*, 2015, **39**, 5931-5935.
18. Y. Chen, C. M. Clouthier, K. Tsao, M. Strmiskova, H. Lachance and J. W. Keillor, *Angew. Chem., Int. Ed.*, 2014, **53**, 13785-13788.
19. W. Ji, G. Liu, M. Xu, X. Dou and C. Feng, *Chem. Commun.*, 2014, **50**, 15545-15548.
20. J. Liu, Y.-Q. Sun, Y. Huo, H. Zhang, L. Wang, P. Zhang, D. Song, Y. Shi and W. Guo, *J. Am. Chem. Soc.*, 2014, **136**, 574-577.
21. J. Luo, R. Uprety, Y. Naro, C. Chou, D. P. Nguyen, J. W. Chin and A. Deiters, *J. Am. Chem. Soc.*, 2014, **136**, 15551-15558.
22. L. He, Q. Xu, Y. Liu, H. Wei, Y. Tang and W. Lin, *ACS Appl. Mater. Interfaces*, 2015, **7**, 12809-12813.
23. J. W. Yan, S. B. Chen, H. Y. Liu, W. J. Ye, T. M. Ou, J. H. Tan, D. Li, L. Q. Gu and Z. S. Huang, *Chem. Commun.*, 2014, **50**, 6927-6930.
24. Y.-Q. Sun, J. Liu, J. Zhang, T. Yang and W. Guo, *Chem. Commun.*, 2013, **49**, 2637-2639.
25. J. Mohanty, N. Barooah, V. Dhamodharan, S. Harikrishna, P. I. Pradeepkumar and A. C. Bhasikuttan, *J. Am. Chem. Soc.*, 2013, **135**, 367-376.
26. A. Renaud de la Faverie, A. Guédin, A. Bedrat, L. A. Yatsunyk and J.-L. Mergny, *Nucleic Acids Res.*, 2014, **42**, e65.
27. N. Amdursky, Y. Erez and D. Huppert, *Acc. Chem. Res.*, 2012, **45**, 1548-1557.
28. L. A. Hanakahi, H. Sun and N. Maizels, *J. Biol. Chem.*, 1999, **274**, 15908-15912.
29. D. Drygin, A. Siddiqui-Jain, S. O'Brien, M. Schwaebe, A. Lin, J. Bliesath, C. B. Ho, C. Proffitt, K. Trent, J. P. Whitten, J. K. C. Lim, D. Von Hoff, K. Anderes and W. G. Rice, *Cancer Res.*, 2009, **69**, 7653-7661.